SUPPORTING INFORMATION

Chemically derived CuO/In$_2$O$_3$ based nanocomposite for diode applications

G. Mohan Kumar[a*], P. Ilanchezhiyan[a], A. Madhan Kumar[b], T. S. Shabi[c],

S. Tamil Selvan[d], S. Suresh[e], Sh. U. Yuldashev[a] and T. W. Kang[a*]

[a]Quantum-Functional Semiconductor Research Center,

Dongguk University, Seoul, Republic of Korea.

[b]Center of Research Excellence in Corrosion,

King Fahd University of Petroleum & Minerals, Kingdom of Saudi Arabia.

[c]Department of Polymer Science and Engineering

Zhejiang University, Hangzhou, China.

[d]Advanced Materials Processing and Analysis Center ,

NanoScience Technology Center, Materials Science Engineering,

University of Central Florida, Orlando, USA.

[e]GT-CNRS-UMI Lab, Georgia Institute of Technology,

2-3, rue Marconi, Metz, France.

Fax: +82-2-2278-4519; Tel: +82-10-4896-1777

Email: gmohankumar@dongguk.edu, twkang@dongguk.edu

Energy-dispersive X-ray spectroscopy (EDS): Thin films of Cu-In-O that were obtained through a traditional drop casting route on glass substrates were used to record the EDS spectrum. The purpose of such examination was to quantify the content of Cu and In elements present in the composite systems. Here, the weight ratio between Cu, In and O elements was found to be 60, 12 and 28 respectively. The analysis was carried out on 2-3 different areas, which hardly revealed any difference in the same.
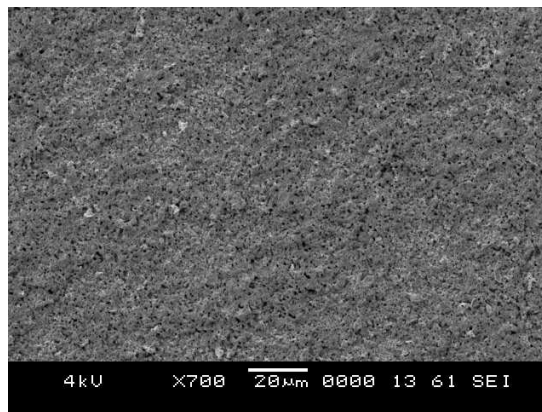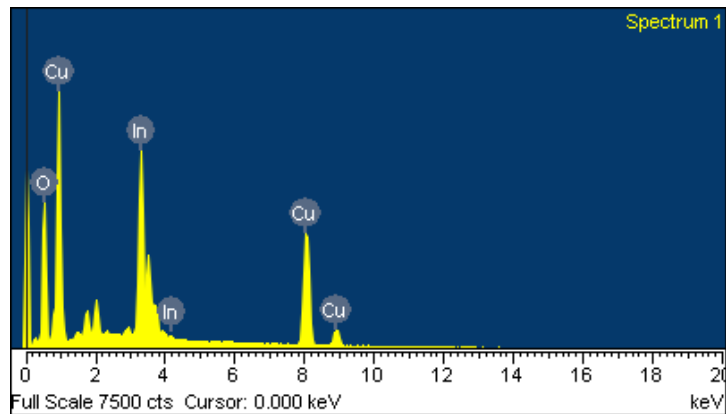

Figure S1: EDS spectrum of Cu-In-O composites and the corresponding area scanned is shown in the SEM image.

Preparation of Cu-In-O dispersions: 10 mg of the processed Cu-In-O powders were initially dispersed in 15-25 ml of ethanol and subjected to sonication for a period of 30 min and subsequently aged for 6-12 h. The ageing process was carried out to separate the larger particulates (through decantation) from the colloidal media. The resulting sol was then used to record the UV-vis absorbance spectrum and for TEM measurements. The same was also used in the fabrication of Cu-In-O made working electrodes and establish p-type active layers on ZnO nanowires *via* drop casting.

Hydrothermal growth of ZnO nanowires: ITO substrates pre-cleaned using acetone; ethanol and deionized water were used to establish the ZnO seed layers *via* immersing the same in a solution made of zinc acetate in ethanol (under stirring for a period of 15 min at 65-70° C). The substrates were then dried in a dry stream of nitrogen gas and annealed at 350° C for 30 min. 3-5 cycles were repeated to obtain uniform deposition of ZnO seed layers. The prepared seed layers were then subjected to hydrothermal treatment in a solution made of 25 mM zinc nitrate and hexamethylenetetramine, respectively. The growth conditions for the nanowires involved their hydrothermal growth at 120° C/3-9 h. The final products were washed with deionized water and annealed at 450° C for 30 min.
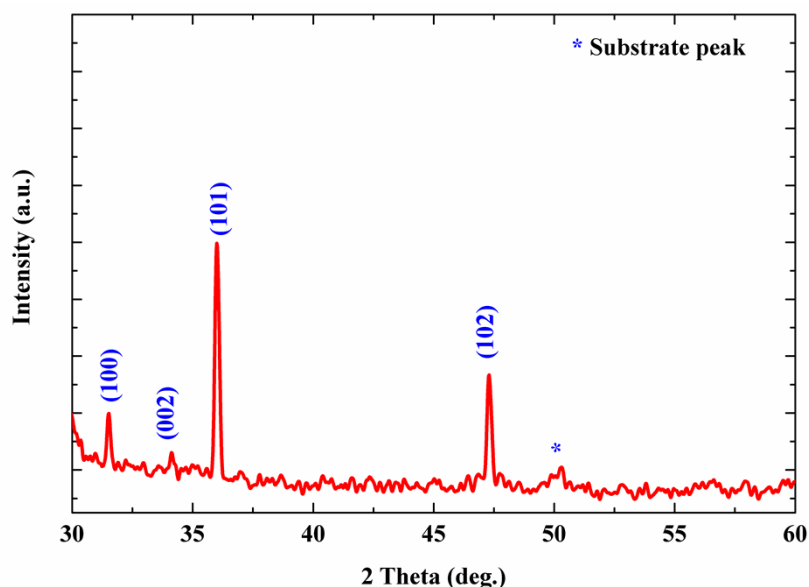

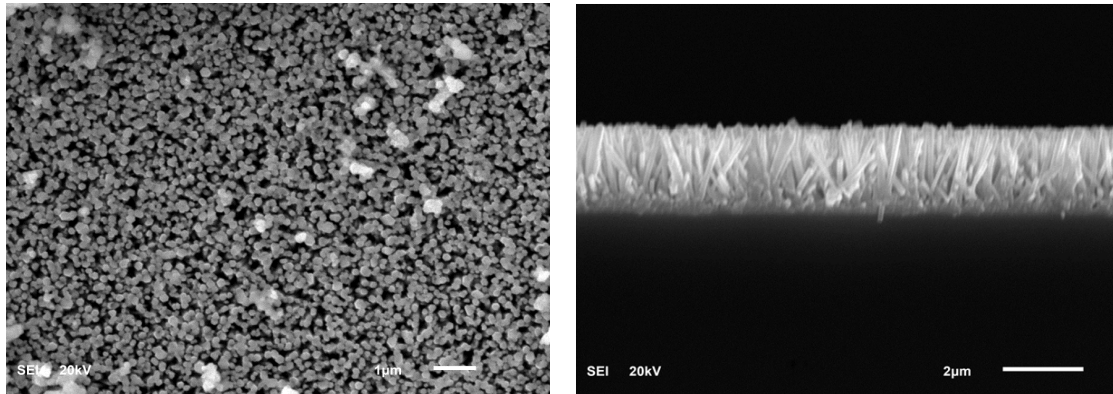**Figure S2:** XRD pattern for ZnO nanowires on ITO.

3

Figure S3: Surface and cross-sectional SEM images revealing the excellent periodicity among the hydrothermally grown ZnO nanowires.

Fabrication of Cu-In-O/ZnO heterostructures: The Cu-In-O made colloidal dispersion was drop casted on the hydrothermally grown ZnO nanowires at room temperature. After the solvents evaporate, the film was heat treated on a hot plate at 150° C for 10 min. Similarly, a maximum of 10 cycles were repeated to attain the active layer with considerable thickness. The resulting heterostructures were finally annealed at 400° C for 30 min, prior to the *I-V* measurements. However, to elucidate the function of thickness of Cu-In-O deposits on the diode behaviour, heterostructures were prepared *via* varying the drop cast cycles in an ascending manner.
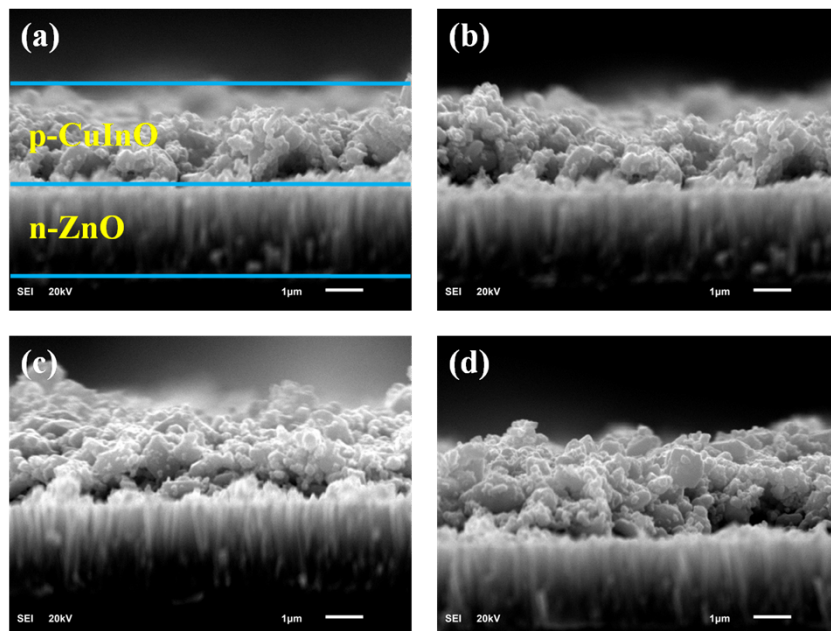

Figure S4: Cross-sectional representation of Cu-In-O/ZnO made p-n heterostructures obtained through (a, b) <5 and (c, d) >5 drop cast cycles.

Charge transfer mechanism in Cu-In-O/ZnO made p-n heterostructures: The schematic energy level diagram proposed in Figure S5 could initially be held responsible for the observed rectification behaviour in the constructed diodes. The schematic layout was actually proposed after considering the existence of CuO and In_2O_3 in form of a blend in the processed Cu-In-O systems. In the proposed step-wise architecture, when the composite material comes in contact with the ZnO nanowires, a p-n junction is naturally established at their heterostructure interface. This favourable band alignment then favours the facile transport of electrons from the conduction band (E_C) of CuO to the E_C of ZnO and the hole transport to take place from the valence band (E_V) of ZnO to the E_V of CuO. Additionally, the In_2O_3 in between CuO and ZnO could also act as an inherent energy barrier and aid with the passivation of surface traps (oxygen vacancies) over the nanowires (caused by the introduction of Cu-In-O). This arrangement might in turn favour the charge transfer kinetics across the device and may be held responsible for the improved rectifying character under illumination. The concept of built-in potential has been additionally discussed in the main text to correlate the improved charge transfer kinetics and rectification behaviour under illumination.
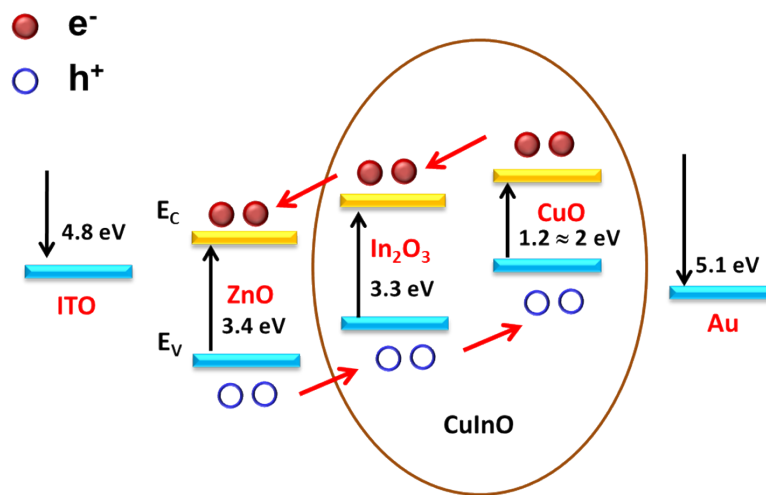

Figure S5: Schematic energy level diagram corresponding to the fabricated heterostructures.

Effect of thickness of Cu-In-O deposits on the I-V performance: The number of drop cast cycles was actually varied during the fabrication of heterostructures to study the influence of thickness of Cu-In-O deposits on the I-V characteristics of Cu-In-O/ZnO made diodes. Figure S6 shows the I-V characteristics that were recorded for the diodes that were fabricated under less than 5 drop cast cycles. Here, the obtained results suggest the constructed devices to produce a higher current under negative bias, affirming the reverse rectifying characteristics under dark and illuminated conditions. The observed characteristics could be attributed to the oxygen related defects, as made clear from the XPS and PL measurements. The extra electrons existing within the oxygen defects might have acted as donor-like states, enabling the realization of an accumulation layer near the interface [1]. This phenomenon in turn could have directed the bands in ZnO to bend downwards, resulting with the e$^-$ accumulation to take place on ZnO side. And, this reverse band bending could have strengthened further under forward bias, thereby restricting the easy flow of carriers and resulting with the observed characteristics.
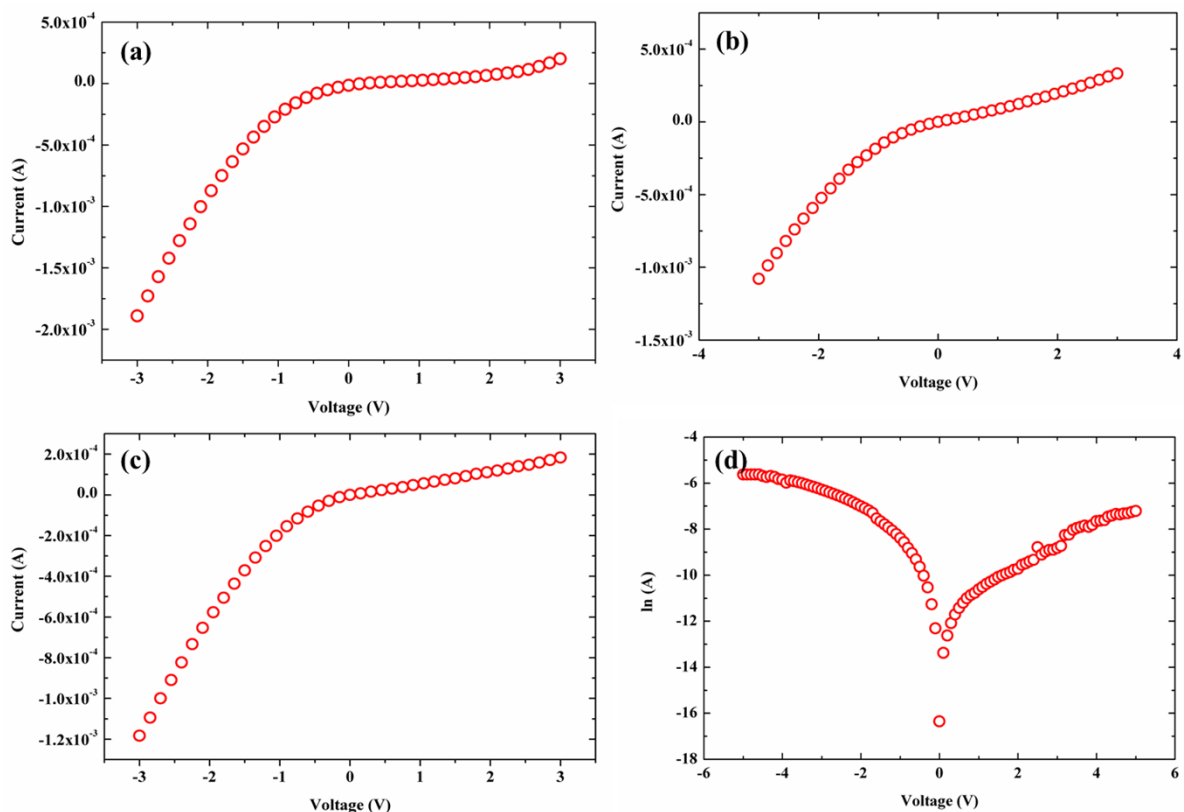

Figure S6: I-V characteristics of Cu-In-O/ZnO made p-n heterostructures that were obtained *via* drop casting the colloidal Cu-In-O suspension on ZnO for <5 times.

I-V characteristics of Cu-In-O/ZnO heterostructures: When the drop cast cycles was held >5, the current values were noted to increase significantly under forward bias and decrease under reverse bias. This behaviour could be attributed to the weakening of reverse band bending, which in turn favours the facile transport of charge carriers across the device structures [2]. The concept of built-in potential is actually discussed in the main script to assimilate the improved rectification properties upon photon illumination.
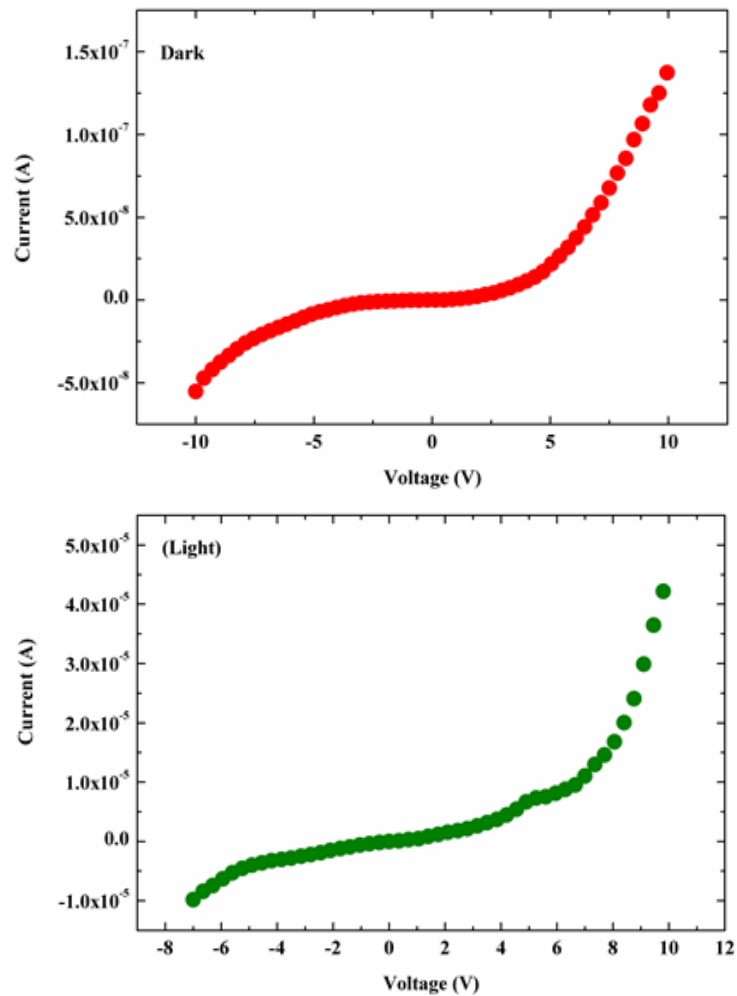

Figure S7: I-V characteristics of Cu-In-O/ZnO made p-n heterostructures that were obtained *via* drop casting the colloidal Cu-In-O suspension on ZnO for >5 times.

Mott-Schottky (MS) plots: The MS plot for D_1 and D_2 i.e. for ZnO and Cu-In-O was studied through a potential scan method under an applied frequency of 100 Hz. The experiments were carried out through exposing 1 cm^2 of the electrode material to a standard phosphate based buffer solution (pH 6/7). Such analysis was used to personify the n-type and p-type conductivity (from the positive and negative slopes) in ZnO and Cu-In-O, respectively [1-4]. The origin of their conductivity could be correlated with the existence of intrinsic defects (such as the negatively charged copper/zinc vacancies or interstitial oxygen) associated within the composite systems. The V_{FB} for the geometrically exposed area was estimated to be around -0.25 and -0.09 V (SCE) for D_1 and D_2, while their corresponding carrier density was calculated to be around 10^{20} and 10^{18} cm^{-3}, respectively.
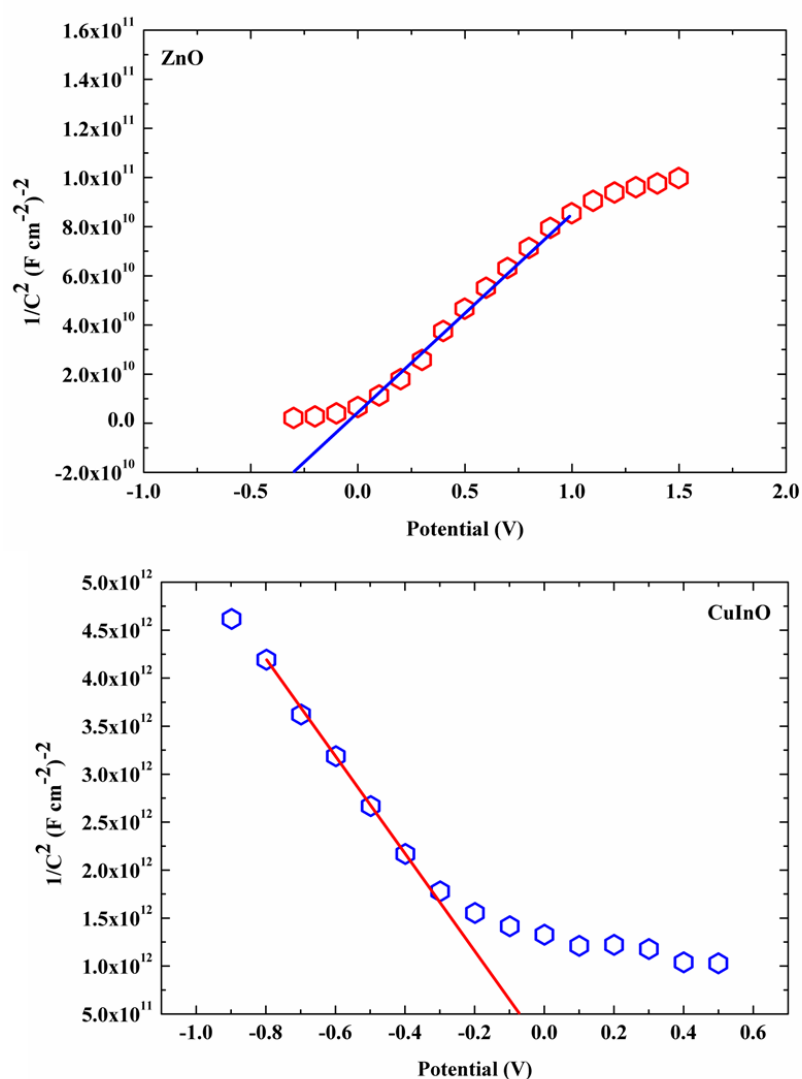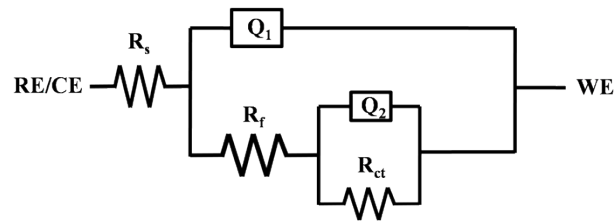

Figure S8: Mott-Schottky (MS) plots signifying the n-type and p-type behaviour in ZnO and Cu-In-O made working electrodes at an applied frequency of 100 Hz.

Impedance measurements: The Nyquist plots obtained for ZnO, Cu-In-O and Cu-In-O/ZnO heterostructures on ITO substrates were fitted individually with an equivalent circuit. The fitting results clearly confirmed the existence of two partial semicircles in all the specimens, one in the lower and the other in the higher frequency region, correspondingly. The best fit parameters have been extracted and provided in the table given below, along with the fitted circuit.

Specimen	R_s kΩ cm²	R_{ct} kΩ cm²	Q_{DL} μA cm⁻²	n	R_f kΩ cm²	Q_F μA cm⁻²	n
ZnO/ITO (D_1)	2.23	373	23.45	0.95	18.52	19.32	0.96
CuInO/ITO (D_2)	3.16	7.850	45.28	0.96	1.223	26.72	0.94
CuInO/ZnO/ITO (D_3)	0.98	29.87	26.43	0.95	7.8	22.32	0.97

Table ST1: EIS best fit parameters obtained through fitting the Nyquist plots (with circuit) obtained for ZnO, Cu-In-O and Cu-In-O/ZnO on ITO.

Here,

WE: Working electrode

RE/CE: Reference and Counter electrodes.

R_s: Solution resistance.

R_f: Primary layer resistance.

R_{ct}: Charge transfer resistance.

Q_F: Constant phase element of primary layer capacitance.

Q_{DL}: Constant phase element of double layer capacitance.

References:

1. U. Diebold, Surf. Sci. Rep., 2003, **48**, 53.

2. K. Bimal Sarma, R. Arup Pal, Heremba Bailung and Joyanti Chutia, J. Phys. D: Appl. Phys., 2012, **45**, 275401.

3. F. Charles Windisch and J. Gregory Exarhos, J. Vac. Sci. Technol. A, 2000, **18**, 1677.

4. A. Wolcott, W. A. Smith, T. R. Kuykendall, Y. Zhao and J. Z. Zhang, Adv. Funct. Mater., 2009, **19**, 1849.

5. O. Musa, T. Akomolafe and M. J. Carter, Sol. Energy Mater. Solar Cells, 1998, **51**, 305.

6. Andreas Othonos and Matthew Zervos, Nanoscale Res. Lett., 2011, **6**, 622.